

1 **DETECTION AND ATTRIBUTION OF FLOOD TRENDS IN MEDITERRANEAN**

2 **BASSINS**

3

4

5

6 Trambly, Yves<sup>1</sup>

7 Mimeau, Louise<sup>1</sup>

8 Neppel, Luc<sup>1</sup>

9 Vinet, Freddy<sup>2</sup>

10 Sauquet, Eric<sup>3</sup>

11

12 <sup>1</sup> HSM (Univ. Montpellier, CNRS, IRD), 300 Av. du Professeur Emile Jeanbrau, 34090,

13 Montpellier, France

14 <sup>2</sup> GRED (Univ. Paul Valéry, IRD), 2 rue du Pr Henri Serres, 34000 Montpellier, France

15 <sup>3</sup> IRSTEA, UR RiverLy, Centre de Lyon-Villeurbanne, 5 rue de la Doua CS 20244, 69625

16 Villeurbanne, France

17

18

19

20

21

22

23 **Version 2, revised manuscript, 20 September 2019**

24

25

26

27

28

29

30

31

32  
33  
34  
35  
36  
37  
38  
39  
40  
41  
42  
43  
44  
45  
46  
47  
48  
49  
50  
51  
52  
53  
54  
55  
56  
57  
58  
59  
60  
61  
62

**Abstract**

Floods have strong impacts in the Mediterranean region and there is a questioning about a possible increase in their intensity due to climate change. In this study, a large database of 171 basins located in South France with daily discharge data with a median record length of 45 years is considered to analyze flood trends and their drivers. In addition to discharge data, outputs of precipitation, temperature, evapotranspiration from the SAFRAN reanalysis and soil moisture computed with the ISBA land surface model are also analyzed. The evolution of land cover in these basins is analyzed using the CORINE database. The trends in floods above the 95<sup>th</sup> and 99<sup>th</sup> percentiles are detected by the Mann-Kendall test and quantile regression techniques. The results show that despite the increase in extreme precipitation reported by previous studies, there is no general tendency towards more severe floods. Only for a few basins, the intensity of the most extreme floods is showing significant upward trends. On the contrary, most trends are towards fewer annual flood occurrences above both the 95<sup>th</sup> and 99<sup>th</sup> percentiles for the majority of basins. The decrease in soil moisture seems to be an important driver for these trends, since in most basins increased temperature and evapotranspiration associated with a precipitation decreases are leading to a reduction of soil moisture. These results implies that the observed increase in the vulnerability to these flood events in the last decades is mostly caused by human factors such as increased urbanization and population growth rather than climatic factors.

**Keywords:**

**Floods, trends, France, Mediterranean, soil moisture**

63

## 64 1. INTRODUCTION

65

66 A number of studies have now established that extreme precipitation could increase due to  
67 climate change in particular in the Mediterranean (Westra et al., 2013, Polade et al., 2017, Ribes  
68 et al., 2018, Trambly and Somot, 2018). Changes in extreme rainfall would be caused by an  
69 increase in the precipitable water content in the atmosphere, related to increasing temperatures,  
70 according to the principle of Clausius-Clapeyron thermodynamics (Drobinki et al., 2016, Pfahl  
71 et al., 2017). Nevertheless, this relationship has a high variability in space, related to temperatures  
72 and available humidity (Prein et al., 2016; Wasko et al., 2016). Several studies observed an  
73 increase in the number of dry days associated with increased rainfall intensities, suggesting that  
74 dry periods in these areas would become longer, but that precipitation could be more extreme  
75 when they occur (Paxian et al., 2015, Polade et al., 2017). Nevertheless, the increase in extreme  
76 rainfall would not offset the decrease in precipitation totals, as the drop in cumulative rainfall  
77 associated with the decrease in the frequency of low to moderate rainfall is expected to  
78 predominate over the gains resulting from the intensification of extreme precipitation (Polade et  
79 al., 2017; 2014).

80

81 Beside changes in precipitation, an increase in rainfall intensity does not necessarily imply an  
82 increase in flood risk (Ivancic and Shaw, 2015, Woldemeskel and Sharma, 2016). Indeed, for a  
83 given rainfall accumulation, the runoff coefficient can be very variable in time and space in  
84 different basins due to complex interactions between precipitation and infiltration processes on  
85 hillslopes which can strongly modulate flood magnitude (Woldemeskel and Sharma, 2016,  
86 Wasko and Sharma, 2017, Bennett et al., 2018). Most global studies on flood trend indicate a  
87 decrease in flood intensity (Do et al. 2017, Wasko and Sharma, 2017, Sharma et al., 2018). Yet,  
88 these trends are highly variable in space for different regions of the globe (Yin et al., 2018, Najibi  
89 and Devineni, 2018). The attribution of these trends is rather uncertain, while Yin et al. (2018)  
90 relate an increase in floods with increased temperatures; Najibi and Devineni (2018) or Hodgkins  
91 et al. (2018) conclude that trends in the flood frequency and duration can be mostly attributed to  
92 long-term climate variability. Nonetheless, as noted by Whitfield (2012), flood generating  
93 processes do not take place at the global but rather a relatively local scale, making generalizations

94 about flooding in future climates difficult and uncertain. For Mediterranean basins, Blöschl et al.  
95 (2017) indicate later winter floods and Mangini et al. (2018) noted a tendency towards increasing  
96 flood magnitude and decreasing flood frequency. These findings are consistent with trends  
97 detected by Mediero et al. (2014) in Spain and Giuntoli et al. (2012) for the South of France.

98  
99 While much work has been done to estimate future climatic conditions, it is not clear about  
100 possible changes in hydrological variables including surface conditions that can strongly  
101 modulate climatic trends (Knighton et al., 2017). In particular, it is known that in many  
102 catchments the initial soil moisture conditions prior to flood events play a key role in flood  
103 generation (Brocca et al., 2008, Trambly et al., 2010, Raynaud et al., 2015, Woldemeskel and  
104 Sharma, 2016, Wasko and Sharma, 2017, Uber et al., 2018, Wasko and Nathan, 2019) and its  
105 temporal change has not been much analyzed up to now. Between two episodes of rain, the base  
106 flow of the perennial rivers originates from the draining of the water contained in the soils and for  
107 some basins from the aquifers. The capacity of the soil to contain water and restore it to generate  
108 runoff depends on its characteristics (e.g. texture, structure, porosity) but also on the amount of  
109 water it already contains at the beginning of a rain episode. Thus, a quasi-saturated soil will not  
110 be able to store a lot of water, which, being unable to infiltrate, will contribute directly to runoff.  
111 In most cases, there is a non-linear relationship between the flow rate and the initial saturation  
112 state of the soil, usually with a threshold value of moisture above which a rapid flow response to  
113 a rainy episode is observed (Norbiato et al., 2008, Viglione et al., 2009, Penna et al., 2011).  
114 Difference in soil types could induce different relationships between floods and initial conditions  
115 (Grillakis et al., 2016, Camarasa-Belmonte, 2016). For intermittent (seasonal runoff only) and  
116 ephemeral streams (runoff only after a rain event), the impact of antecedent soil moisture is more  
117 complex and strongly dependent on the soil type and geological context (in the presence of karst  
118 in particular). In smaller basins, the impact of initial soil moisture content is usually not  
119 significant and it increases with catchment size (Zhang et al., 2011).

120  
121 For some Mediterranean basins, the increase in heavy rainfall associated with a reduced number  
122 of rainy days could decrease the soil water content and therefore increase infiltration capacity,  
123 hence reducing runoff. On the other hand, more intense rains in urbanized, impervious areas or  
124 on bare soils that are subject to crusting effects could increase runoff and therefore the magnitude

125 of floods. It is therefore necessary to use hydrological or surface models capable of representing  
126 these processes. Quintana-Seguí et al. (2011) using the ISBA land surface scheme with different  
127 downscaling methods found a future increase in floods corresponding to a 10-year return level in  
128 southern French basins, but with different magnitudes depending on the basins. Camici et al.  
129 (2017), in a study on the impacts of climate change on floods in central Italy, noted a greater  
130 sensitivity of basins with permeable soils to changing climatic conditions. Similarly, Piras et al.  
131 (2017) in Sardinia found that impermeable and flat sub-basins are predicted to experience more  
132 intense flood events in future scenarios, while more permeable and steep sub-catchments will  
133 have an opposite tendency. However, there are systematic differences between projections of  
134 changes in flood hazard in south Europe (Italy, Greece, Iberian Peninsula) in most European and  
135 global studies using large-scale hydrological models (Kundzewicz et al., 2017). Indeed some  
136 studies points towards an increase in southern Europe (Quintana-Seguí et al., 2011, Alfieri et al.,  
137 2015) while others suggests a decrease (Donnelly et al., 2017, Thober et al., 2018). This is due to  
138 different GCM, RCM, scenarios and downscaling approaches but also the use of large scale  
139 hydrological model usually not calibrated and validated for all basins. This type of global (or  
140 large scale) hydrological model (e.g. LISFLOOD, VIC, HYPE) is usually not adapted to small  
141 river basins less than 500 km<sup>2</sup>, which is the typical catchment size found in the Mediterranean  
142 region.

143  
144 Prior to make future projections on flood hazard, there is a need to understand the main drivers of  
145 changes for floods and the links between floods and climate characteristics (Merz et al., 2014).  
146 Indeed, understanding the potential flood drivers and their changes may be more relevant than  
147 predictions of uncertain flood changes as noted by Blöschl et al. (2016, 2015). The objective of  
148 this study is to analyze trends in floods characteristics for a large sample of French Mediterranean  
149 basins and to relate these trends to climate and land use dynamics. This is done using statistical  
150 tests for the detection of trends and quantile regression models to relate high discharge quantiles  
151 to different climatic drivers.

152

## 153 2. DATA

154

155 171 basins located in south France are selected with a minimum of 20 years of daily discharge  
156 data. The selection of basins is based on the availability of long time series of daily discharge and  
157 the selected basins have no significant human influence on flow, from a previous database  
158 elaborated from Sauquet and Catalogne (2011) and Snelder et al. (2013). The median record  
159 length is 45 years and 56 stations have more than 50 years of data, more than 100 stations have  
160 complete years, with less than 5% missing data, between 1970 and 2010. All the catchments  
161 selected have a Mediterranean climate, with a precipitation deficit during summer when the low  
162 flows are recorded. These basins are experiencing flash flood events caused by intense rainfall  
163 events, corresponding to the only region in France when rainfall can exceed 200 mm/day  
164 (<http://pluiesextremes.meteo.fr>) with the maximum occurrence between September and  
165 November. Most basins have a catchment area lower than 500 km<sup>2</sup> and located below 1000 m.  
166 (figure 1). The proportion of karstic areas for each basin has been obtained from the BDLISA  
167 database (available here: <https://bdlisa.eaufrance.fr/>) which provides a delineation of karst  
168 systems in France (Schomburgk et al., 2016). Very common geological formation in the French  
169 Mediterranean region, about 50 gauged basins have more than 50% of their catchment areas with  
170 carbonaceous superficial formations, indicative of Karstic areas. This means that the rainfall-  
171 runoff relationship in this type of basin can be strongly modulated by the presence of karst  
172 (Jourde et al., 2007).

173  
174 In addition to daily discharge data, different ~~climatic~~-variables have been retrieved from the  
175 ~~SAFRAN-ISBA-MODCOU (SIM) hydro-meteorological model (Habets et al., 2008). SIM is~~  
176 ~~based on the~~ SAFRAN reanalysis over France (Quintana-Seguí et al., 2008) ~~based~~. ~~This~~  
177 ~~reanalysis-based~~ on observed ~~station~~-data ~~and~~ provides rainfall, snowfall, temperature, ~~actual~~-and  
178 reference evapotranspiration for a 8x8km grid over France at the daily time step from 1958 until  
179 present. The SAFRAN reanalysis is used to force the ISBA land surface scheme of Météo-France  
180 (Habets et al., 2008), to provide among other variables the ~~actual evapotranspiration, the~~ surface  
181 and root zone soil moisture at the same spatial and temporal resolution than ISBA. Trambly et  
182 al. (2010) have shown that the soil moisture from the root zone simulated by ISBA is an  
183 appropriate indicator of soil moisture prior to flood events in French Mediterranean catchments.  
184 The catchment boundaries of the 171 basins selected have been extracted from the HydroSheds  
185 database (<https://hydrosheds.org/>) providing flow accumulation and flow direction maps at the 15

186 arc-second resolution. Then the total precipitation, rainfall, air temperature, actual and reference  
187 evapotranspiration from SAFRAN and the surface and root zone soil moisture from ISBA have  
188 been extracted and averaged over every catchment.

189  
190 The evolution of landcover between 1990 and 2018 in the 171 basins was analyzed using the  
191 Corine Landcover inventory (CLC1990 and CLC 2018). Corine Landcover provides an inventory  
192 of 44 classes over the European region (Büttner et al., 2002). CLC1990 and CLC2018 are  
193 respectively based on Landsat-5 (50m spatial resolution) and Sentinel-2 (10m spatial resolution)  
194 satellite images. A limitation of the CLC inventory lies in the difference of accuracy between the  
195 CLC1990 and CLC2018 products, which may introduce an uncertainty in the estimation of the  
196 evolution of the land cover in the studied basins.

197

### 198 **3. METHODS**

199  
200 Two approaches are considered to evaluate trends. The first approach, presented in section 3.1  
201 thereafter, relies on the Mann-Kendall test ([Mann 1945](#)) applied to the annual number of flood  
202 events above two different percentiles, the 95<sup>th</sup> and the 99<sup>th</sup> computed on the whole time series  
203 and also on the magnitude of these events. Using two different thresholds, which are commonly  
204 used for the analysis of floods, allows considering separately the trends on moderate (above the  
205 95<sup>th</sup> percentile) and more severe (above the 99<sup>th</sup> percentile) flood events.

206  
207 The second approach presented in section 3.2, is based on quantile regression ([Koenker and](#)  
208 [Basset, 1978](#)) to estimate the temporal trend magnitude in the 95<sup>th</sup> and 99<sup>th</sup> percentiles of daily  
209 runoff in all stations. The quantile regression method is also used to relate the change in runoff  
210 quantiles to changes in climate characteristics, hence providing a way to attribute the observed  
211 changes to their potential drivers.

212  
213 Hydrological years are considered, starting September 1<sup>st</sup> and ending August, 31 of the next  
214 calendar year. Years with more than 5% missing days are removed. For the first approach based  
215 on event characteristics, a de-clustering is required to not include in the flood sample consecutive  
216 daily threshold exceedances that belong to the same flood event. A minimum of 2 days between

217 two flood events is selected since it is the average duration of rainstorm in the region (Tramblay  
218 et al. 2013). This means, if for two consecutive days the runoff is exceeding the threshold, only  
219 the maximum value is retained. Moreover, different values between 1 and 5 days to separate the  
220 events have been tested ~~but preliminary tests indicated that it~~ and did not change the trend results.

221

### 222 3.1 Test for trends and regional significance

223

224 The Mann–Kendall (MK) test (Mann 1945) is used for the trend detection. Several studies have  
225 noted that the presence of serial correlation may affect the results of trend analysis by increasing  
226 the variance of the test statistic (Khaliq et al., 2009, Renard et al., 2008). To overcome this  
227 limitation, Hamed and Rao (1998) proposed a corrected MK test statistic considering an effective  
228 sample size that reflects the effect of serial correlation. This correction was applied in the present  
229 study. In addition to the MK test, the method of Sen (1968) is considered to estimate the  
230 magnitude of trends. In the present study, trends are considered significant at the 10% level;  
231 however, sensitivity tests performed for  $p \leq 0.05$ ,  $p \leq 0.01$  revealed very similar spatial trend  
232 patterns.

233

234 The significance level  $\alpha_{\text{local}}$  for a statistical test is related to a single test and is no longer valid  
235 when multiple tests are conducted (Wilks 2016). When the number of tests being conducted  
236 increases, more significant values will be found. The goal of the false discovery rate (FDR)  
237 procedure introduced by Benjamini and Hochberg (1995) is to identify a set of at-site significant  
238 tests by controlling the expected proportion of falsely rejected null hypotheses that are actually  
239 true. Renard et al. (2008), Khaliq et al. (2009) or Wilks (2016) demonstrated that the original  
240 FDR is robust to cross correlations between locations and can work with any statistical test for  
241 which one can generate a p-value. This FDR method is applied to the MK test results to check if  
242 the trends are regionally significant. The detected trends are regionally significant if at least one  
243 local null hypothesis is rejected according to the global (or regional) significance level,  $\alpha_{\text{global}}$   
244 (Wilks, 2016). For consistency with the local trend analysis, the global significance level is also  
245 set to 10% in the FDR procedure.

246

### 247 3.2 Quantile regression



248  
249 As a complementary approach to detect trends in quantiles but also to investigate the relationship  
250 between floods and explanatory covariates, the quantile regression (Koenker and Bassett, 1978)  
251 method is applied. Quantile regression could be seen as the extension of the ordinary least square  
252 (OLS) regression (Koenker and Machado, 1999, Villarini and Slater 2017). In OLS, the  
253 conditional mean of the response variable is modeled with respect to one or more predictors and  
254 the sum of squared errors is minimized. For quantile regression, a conditional quantile of the  
255 response variable is modelled as function of predictor(s), an asymmetrically weighted sum of  
256 absolute errors is minimized to estimate the slope and intercept terms. In the present work, only  
257 linear relationships are considered with one single covariate at a time, while more complex forms  
258 of dependences could also be considered in quantile regression. The approach has been  
259 previously used to detect trends in extreme precipitation or floods by Villarini and Slater (2017),  
260 Yin et al. (2018) or Wasko and Nathan (2019).

261  
262 Koenker and Machado (1999) introduced the  $R^l$  goodness of fit measure for quantile regression  
263 models. As for the  $R^2$  in the case of OLS,  $R^l$  lies between 0 and 1. Unlike  $R^2$ , which measures the  
264 relative success of two models for the conditional mean function in terms of residual variance,  $R^l$   
265 measures the relative success of the corresponding quantile regression models for a specific  
266 quantile, by comparison with a restricted model (with slope = 0), in terms of a weighted sum of  
267 absolute residuals (see Koenker and Machado, 1999). Consequently,  $R^l$  constitutes only a local  
268 measure of goodness-of-fit for a particular quantile rather than a global measure over the entire  
269 conditional distribution, like  $R^2$ . This measure can help to discriminate between different models  
270 using different covariates (ex: precipitation or temperature). Higher  $R^l$  values indicate that the  
271 model fits better to observations. In this study, this criterion is used to identify the best covariates  
272 that could explain the temporal variations in high runoff quantiles.

273

## 274 **4. RESULTS**

275

### 276 **4.1 Climatic and land cover trends**

277

278 The climate trends have been analyzed on the whole period of available SAFRAN records,  
279 between 1958 and 2018. For each basin, the annual trends in precipitation, rainfall, temperature,  
280 soil moisture, actual and reference evapotranspiration have been analyzed with the Mann Kendall  
281 test. From figure 2, It can be seen a significant decrease of annual rainfall in 56 basins, on  
282 average of -20%, accompanied by an increase of the frequency in dry days (with precipitation  
283 below 1 mm) for 46 basins. The snowfall is also decreasing in the same proportions (no shown).  
284 The sole exception where an increase in rainfall is found is for the Asse River at Beyne-  
285 Chabrières on the western foothills of the Alps. This station has long time series spanning from  
286 1983 to 2009, where a +15% trend in annual rainfall is detected over the whole record. Yet, the  
287 detection of this trend might be an artefact since there are several consecutive wet years between  
288 1992 and 2000. This trend in rainfall can be also seen for the soil moisture trends. Associated  
289 with the precipitation decrease, positive temperature trends are observed for almost all basins,  
290 with an average increase of +0.5°C during the time period 1958-2015. Consequently, widespread  
291 increasing trends in reference and actual evapotranspiration rates over all basins are observed,  
292 similarly as in Vicente-Serrano et al. (2014) in Spain or Rivoire et al. (submitted2019) for the  
293 whole Mediterranean region. The combined decrease in precipitation with increased  
294 evapotranspiration yields to a decrease in soil moisture for the surface and the root zone layers.  
295 Yet, it must be stressed here that the soil moisture in the present study is not observed but  
296 simulated from the ISBA land surface model. However, the detected trends are~~This is~~ in  
297 accordance with previous studies over South France such as Vidal et al. (2012) or Dayon et al.  
298 (2018).

299  
300 About land cover (figure 3), most basins have low urban areas (below 10%) and the basins with  
301 the highest coverage are found mostly in the South East. An increase of urban areas up to +20%  
302 of total catchment surface can be seen between 1990 and 2018 for basins mostly located close to  
303 the Mediterranean coast and in particular in the Provence-Alpes-Côte-d'Azur region. The class  
304 representing discontinuous urban fabric represents 73% of artificialized areas and increased by  
305 +36% between 1990 and 2018. The increase of urbanized areas could have a strong impact on  
306 runoff generation, in particular for small basins, with the increase of impervious surfaces favoring  
307 surface runoff. In contrast, the agricultural and forest land cover can reach 100% of the basin  
308 surface, in particular in the western Tarn regions for agriculture. We can notice a reduction of

309 forest cover in the Northern Cévennes areas associated with an increase in agricultural surfaces.  
310 When looking in details from the original classification, for some catchments of size 500 km<sup>2</sup> or  
311 less, the percentage of vineyards could exceed 70% of the total catchment areas in particular for  
312 basins located in the Occitanie region. For almost all basins, the percentage of vineyards has  
313 decreased between 1990 and 2018. The other dominant land use classes related to agriculture are  
314 pastures (27.8% of all catchments), complex cultivation patterns (21.9%) and land principally  
315 occupied by agriculture with significant areas of natural vegetation (27.7%). Forested areas are  
316 mostly represented by broad-leaved forest (35%), coniferous forest (19%) and mixed forest  
317 (14.4%) classes. It must be noted that the land cover change analysis is hampered by the short  
318 duration of the land use maps available, 28 years between 1990 and 2018, and possibly different  
319 sensors during this period leading the different attribution to some land use classes.

320

## 321 4.2 Flood trends

322

323 To analyze flood trends, all flood events above the 95<sup>th</sup> or 99<sup>th</sup> percentiles of daily runoff  
324 computed on the whole time series are extracted. As noted in the method section, a declustering  
325 approach has been implemented to avoid introducing in the samples an autocorrelation signal due  
326 to several consecutive threshold exceedances belonging to the same event. The trend MK test is  
327 applied to the number of annual exceedances above these two thresholds and also on the  
328 magnitude of the threshold exceedances. From figure 4 it can be seen a general tendency towards  
329 a decrease in the annual number of flood events above the 95<sup>th</sup> percentile, that is significant in 67  
330 catchments, and to a lesser extend also in the number of events above the 99<sup>th</sup> percentile in 45  
331 catchments. These trends are regionally significant according to the FDR procedure and  
332 particularly over the northern ridge of the Cévennes mountainous areas. According to the Sen  
333 Slope method to estimate the decrease in the annual number of events above the 95<sup>th</sup> percentile;  
334 for most basins the trends are ranging between -0.5 and -1 event per decade. For the most  
335 extreme cases the trends can reach up to -2.5 events per decade. Since for all catchments the  
336 number of events above the 95<sup>th</sup> percentile per year is 4.5 on average (min =2, max =6, after de-  
337 clustering), the magnitude of these trends can be considered low/moderate. For the 99<sup>th</sup> percentile  
338 the magnitude of trends are similar, with a maximum decrease of -1.4 events per decade, and for  
339 most stations on average -0.4 events per decade (with an average annual number of 1.6 events

340 above the 99<sup>th</sup> percentile, after de-clustering). In addition to the trends in the annual number of  
341 events, there is also a weak signal of an increase of the magnitude of floods, in particular above  
342 the 99<sup>th</sup> percentile for 16 stations, yet these trends are not regionally significant.

343  
344 Beside this event-based analysis, the temporal trends in the 95<sup>th</sup> and 99<sup>th</sup> percentiles of the daily  
345 runoff time series have been investigated using quantile regression. The approach is  
346 complementary but different to the testing of trends on the annual occurrence and the magnitude  
347 of the events, since quantile regression allows evaluating the possible changes on the quantiles of  
348 daily runoff time series. This analysis reveals that for a majority of catchments, a decreasing  
349 trend in these two percentiles is detected. The procedure is to apply a quantile regression of the  
350 percentile of interest with time as a covariate, and to validate if the slope of the quantile  
351 regression model is significantly different than zero at the 10% level a bootstrap resampling  
352 approach (Efron, 1979) has been considered. For the 95<sup>th</sup> percentile, a decreasing trend in 147  
353 stations is found and an increase in only 12 stations. For the 99<sup>th</sup> percentile, 89 negative trends  
354 are found and 15 stations with increasing trends. The relative changes in the 95<sup>th</sup> and 99<sup>th</sup>  
355 percentiles are ranging for most stations between 0 and -0.5 as shown on figure 5. The number of  
356 detected trends with quantile regression for the 95<sup>th</sup> and 99<sup>th</sup> percentiles is larger than the number  
357 of trends detected with the MK test. However, for many basins the trends in the 95<sup>th</sup> and 99<sup>th</sup>  
358 percentiles are of small magnitude and only for the largest trends the MK test also detect  
359 significant changes in the annual number of events above these thresholds.

360  
361 In an attempt to relate the detected trends to catchment characteristics, the Student t-test has been  
362 used to compare the catchment descriptors between the group of basins with or without trends.  
363 The catchments where decreasing trends in flood occurrence are detected tend to be are larger  
364 catchments (mean size of 369 km<sup>2</sup> vs. 253 km<sup>2</sup> for the catchments with no significant trends),  
365 with a lower proportion of karstic areas (33% vs. 41%) and urban areas (1.7% vs 3.79%). Also  
366 more decreasing trends are detected in agricultural catchments than in forested areas. Yet, no  
367 clear link can be found between land cover changes and flood trends, probably due to the short  
368 duration of the land cover dataset available. The only exception is about trends in urbanization,  
369 with a lower increase in urbanization (+0.77% average increase in urban areas) in catchments  
370 where floods are decreasing by comparison with catchments with no flood trends (+1.41%

371 average increase in urban areas). It must be noted that there is a strong spatial variability of the  
372 observed trends highlighting the complex interplays between the different catchment  
373 characteristics, as similarly noted by Snelder et al. (2013) over France. For example, the  
374 magnitude of the detected trends is not correlated with the different catchment properties. This  
375 implies that it would be very challenging to propose a typology of basins with similar changes in  
376 floods according to catchment properties.

377

### 378 **4.3 Changes in event precipitation and antecedent soil moisture conditions**

379

380 For each event, the cumulative catchment precipitation average is computed as the sum of non-  
381 zero consecutive rainy days, on a time window up to 10 days prior to the flood event. The  
382 antecedent soil moisture is taken as the root zone soil moisture corresponding to the day prior the  
383 start of the rainfall event. Figure 6 show the Mann-Kendall test results for these two indicators for  
384 floods above the 95<sup>th</sup> and the 99<sup>th</sup> percentiles. An increase of precipitation associated with floods  
385 using both thresholds is observed (for 34 catchments for the 95<sup>th</sup> percentile and 36 catchments for  
386 the 99<sup>th</sup> percentile), associated with a decrease in antecedent soil moisture conditions prior to  
387 floods in up to 40 catchments for floods above the 95<sup>th</sup> percentile. There is a correlation between  
388 the reduction of antecedent soil moisture prior to flood events and the decrease of the annual  
389 number of flood events above the 95<sup>th</sup> percentile ( $r=0.44$ ), also to a lesser extent for the number  
390 of floods above the 99<sup>th</sup> percentile ( $r=0.34$ ). Consequently, as observed in Australia by Wasko  
391 and Nathan (2019) it can be hypothesized that the decrease of antecedent soil moisture is an  
392 important driver leading to the reduction of the annual number of floods, despite the increase in  
393 event precipitation already pointed out by several studies in this region (Tramblay et al., 2013,  
394 Ribes et al., 2018, Blanchet et al., 2018). Indeed, for 12 catchments an increase of event rainfall  
395 is detected when for the same catchments a decrease in the annual number of events above the  
396 95<sup>th</sup> percentile is also observed. It is also the case of 11 catchments for the events above the 99<sup>th</sup>  
397 percentile with an increase of event rainfall accompanied by a decrease in the annual number of  
398 events. However as shown before, the increased event precipitation for several basins is probably  
399 the cause of higher flood magnitudes for the most severe events (above the 99<sup>th</sup> percentile).

400

### 401 | **4.3.4 Explanatory covariates for high runoff quantiles**

402  
403 To test the influence of different covariates on the variation of the 95<sup>th</sup> and 99<sup>th</sup> percentile values,  
404 quantile regression models using time, temperature, soil moisture from the root zone, actual  
405 evapotranspiration (AE), reference evapotranspiration (ET0) and precipitation have been  
406 compared. The goal here is not to select the best covariates for each station but to identify  
407 relevant covariates at the regional scale. Since climatic covariates could influence the  
408 hydrological response at different time scales (Mediero et al., 2014, Villarini and Slater 2018,  
409 Wasko and Nathan, 2019), three different aggregation periods to compute moving averages have  
410 been compared. For the event scale, the different covariates have been averaged with a 3-day  
411 time lag preceding each event. At the monthly time scale representing the seasonal variability, the  
412 covariates have been averaged for the 30 days preceding the events. For the annual time scale the  
413 covariates have been averaged for 365 days preceding the events. At the monthly time scale  
414 representing the seasonal variability, the covariates have been averaged in the same manner but  
415 on 30 days. Finally, for the annual time scale the covariates have been averaged over 365 days.  
416 At the event scale, the precipitation ~~rather~~ represents the intensity of rainfall during the event than  
417 the preceding soil moisture. On the ~~opposite~~other timescales, for the monthly and annual  
418 aggregation periods the precipitation is here a proxy for soil moisture and its long term  
419 variability. To test which covariate provides the best reproduction of the observed 95<sup>th</sup> and 99<sup>th</sup>  
420 percentiles of the daily discharge time series, the  $R^I$  metric is computed, for each covariate,  
421 between the quantile regression model built with the covariate and a constrained model with a  
422 constant slope (0).

423  
424 The results are plotted on figure 9. A similar pattern can be seen for both percentiles, with  
425 decreasing  $R^I$  values for longer time aggregation periods for the covariates. For the event-scale,  
426 both precipitations and soil moisture are outperforming other covariates, including time. The  
427 same results are found for the annual time scale, yet with a different interpretation because annual  
428 precipitation is representing the average level of soil moisture storage rather than event rainfall.  
429 The link observed between the 95<sup>th</sup> and 99<sup>th</sup> percentiles with annual precipitation or soil moisture  
430 is an indication that the long-term decrease observed for these two variables (figure 2) could be  
431 the cause of the observed decrease in the frequency of floods above these two percentiles. At the  
432 monthly time scale, the cumulative precipitation plays the most important role when the effects of

433 soil moisture, actual evapotranspiration and temperature are similar. For almost all covariates,  
434 there is an improvement by comparison to the quantile regression model using time only.

435  
436 Overall, the  $R^I$  coefficients are decreasing with increasing slopes and basin mean  
437 ~~attitude~~elevation. However, these two variables are correlated ( $r=0.61$ ). This is an indication that  
438 antecedent soil moisture condition may have a lower influence on flood generation in  
439 mountainous areas, probably due to shallower soils and steeper slopes. For event based soil  
440 moisture and precipitation, there is an inverse relationship with basin size: for small basins (less  
441 than 500km<sup>2</sup>) event soil moisture and precipitation are ~~very~~ good predictors for the time  
442 variations of the 95<sup>th</sup> and the 99<sup>th</sup> percentiles, with  $R^I$  values up to 0.6, when for larger basins the  
443  $R^I$  values are much lower, reaching a maximum of 0.2 for some basins. ~~(about 0.1 to 0.2)~~. When  
444 averaged at the monthly or annual time step, the relation is opposite with a larger influence of soil  
445 moisture and antecedent precipitation for larger basins with higher  $R^I$  coefficients. This finding is  
446 fully consistent with results obtained for different regions of the globe (Zhang et al., 2011,  
447 Ivancic and Shaw, 2015, Woldemeskel and Sharma, 2016, Wasko and Sharma, 2017),  
448 highlighting the buffering effects of large basins with the capacity to store more water than  
449 smaller basins.

450

## 451 5. CONCLUSIONS

452  
453 The results obtained in the present study show that despite the increase in extreme precipitation  
454 events reported by previous studies over the same domain (Ribes et al., 2018) there is not a  
455 general increase in flood occurrence. Only for a few basins, the intensity of the most extreme  
456 floods is showing significant upward trends. On the contrary, a global tendency towards fewer  
457 annual flood occurrences is observed for events of moderate intensity, above the 95<sup>th</sup> percentile.  
458 The same signal, with a lower magnitude, is also seen for higher floods above the 99<sup>th</sup> percentile.  
459 Overall, there are much more trends detected for the annual occurrence of floods than for their  
460 intensity. It should be also emphasized that the magnitude of these trends remains moderated,  
461 with only a few events less by decade and consequently these trends are only noticeable over  
462 long time periods. The decrease in soil moisture seems to be an important driver for these  
463 detected changes, indeed in all basins an increase of temperature and evapotranspiration

464 associated with a decrease in precipitation is leading to a reduction of soil moisture over time. For  
465 several basins, the soil moisture decrease can offset the increase in extreme precipitation and  
466 generate less frequent floods. These changes are mostly observed for larger agricultural basins,  
467 with low urbanization and karstic areas. Wasko and Sharma et al. (2017) previously noted the  
468 importance of catchment size for the influence of soil moisture on flood runoff due to higher  
469 potential of soil moisture storage. The trends detected in the present work are consistent with  
470 those found in other Mediterranean regions such as Spain (Mediero et al., 2014) and Australia  
471 (Wasko and Nathan, 2019). An important finding of the present work is that with the same large  
472 scale climatic drivers (in terms of temperature, evapotranspiration and precipitation) the flood  
473 trends in the basins can be different. This shows the importance of basins characteristics to buffer  
474 climatic variability. Indeed, even if similar patterns of changes in the 95<sup>th</sup> and 99<sup>th</sup> percentiles are  
475 found, the analysis of individual catchments is revealing spatial differences even for neighboring  
476 basins caused by different topography, soil and land cover combinations. This is a factual  
477 demonstration of the commentary of Whitfield (2012) stating that it would be very difficult, if  
478 not scientifically irrelevant, to make general statements about the plausible future evolution of  
479 flood risk.

480  
481 These results showing a lack of a generalized upward trend in floods should be put into  
482 perspective with the observed increase in the vulnerability to these episodes. Indeed many reports  
483 such as Llasat et al (2013) indicate an increase in the number of floods inducing damages  
484 between 1981 and 2010 in South France and North Spain, which they attribute to an increased  
485 vulnerability and land use changes. The French Mediterranean regions are concentrating 66% of  
486 the total cost of flood damage to private properties in France (Vinet, 2011) and the total assets  
487 lost due to floods are rising as in many other regions (CCR, 2018, Paprotny et al., 2018). The  
488 areas close to the Mediterranean have seen a population increase and an extension of urbanized  
489 areas, driven in part but not solely by the increase of touristic activities (Vinet, 2011, Vinet and  
490 De Richemond, 2017). Boucher (2011) concluded after a review of 22 disaster loss studies that  
491 there is no trends in flood losses, corrected for changes (increases) in population and capital at  
492 risk, which could be attributed to anthropogenic climate change". Therefore, it can be concluded  
493 that, at least for Southern France, as noted previously by Neppel et al. (2003) the increasing cost  
494 of damages caused by floods is rather due to the increase in socio-economic vulnerability rather



495 than a climate change signal towards an increase in the severity of floods. Nonetheless, the  
496 evolution of flood frequency and intensity is a key question for risk prevention. Flood related  
497 mortality in the Mediterranean basin is conditioned both by hazards drivers (e.g. rainfall  
498 intensity, discharge~~---~~) but also by social drivers (behaviors, characteristics of buildings...) as  
499 shown in different studies (Ruin et al., 2008, Vinet, 2011, Boudou et al., 2016). Deeper  
500 knowledge in rainfall and flood trends must be crossed with exposure (e.g. population in flood  
501 prone zones) and vulnerability data (e. g. eldering of population in the future) to anticipate  
502 evolution in human mortality in relation with flash floods in the Mediterranean basin (Petrucci et  
503 al. 2017). As pointed out in previous research projects (Merz et al., 2014, Meyer et al., 2014)  
504 there is a need to integrate climate change scenarios with socio-economic change scenarios to  
505 better quantify changes in flood risk. To achieve this task, it is necessary to develop databases on  
506 vulnerability and exposure to be analyzed in conjunction with hydrometeorological data (Saint-  
507 Martin et al., 2018).

508

#### 509 **Acknowledgements**

510

511 This work is a contribution to the HYdrological cycle in The Mediterranean EXperiment  
512 (HyMeX) program, through INSU-MISTRALS support. The dataset compiled in this work  
513 are made available to the research community upon request.

514

#### 515 **References**

516

517 Alfieri, L., Burek, P., Feyen, L., and Forzieri, G.: Global warming increases the frequency of river floods  
518 in Europe, *Hydrol. Earth Syst. Sci.*, 19, 2247-2260, <https://doi.org/10.5194/hess-19-2247-2015>, 2015.

519

520 Benjamini, Y. and Hochberg, Y.: Controlling the false discovery rate: A practical and powerful  
521 approach to multiple testing, *J. Roy. Stat. Soc. B*, 57, 289–300, 1995.

522

523 Bennett B., Leonard, M., Deng Y., and Westra, S.: An empirical investigation into the effect of antecedent  
524 precipitation on flood volume, *J. Hydrol.*, 567, 435-445, 2018.

525

526 Blanchet, J., Molinié, G., and Touati, J.: Spatial analysis of trend in extreme daily rainfall in southern  
527 France, *Clim Dyn.*, 51, 799-812, 2018.

528

529 Blöschl, G., Gaál, L., Hall, J., Kiss, A., Komma, J., Nester, T., et al.: Increasing river floods: fiction or  
530 reality? *WIREs Water*, 2, 329–344, 2015.

531

532 Blöschl, G., Hall, J., Parajka, J., Perdigão, R.A., Merz, B., Arheimer, B., et al.: Changing climate shifts  
533 timing of European floods, *Science*, 357, 588–590, 2017.

534

535 Boudou, M., Lang, M., Vinet, F., and Cœur, D.: Comparative hazard analysis of processes leading to  
536 remarkable flash floods (France, 1930–1999), *J. Hydrol.*, 541, 533–552, 2016.

537

538 Bouwer, L. M.: Have disaster losses increased due to anthropogenic climate change? *Bull. Am. Met. Soc.*  
539 92 (1), 39-46, 2011.

540

541 Brocca, L., Melone, F., and Moramarco, T.: On the estimation of antecedent wetness conditions in  
542 rainfall–runoff modelling, *Hydrol. Processes*, 22, 629–642, 2008.

543

544 [Büttner, G., Feranec, F., and Jaffrain, G.: Corine land cover up-date 2000. Technical report,](#)  
545 [Copenhagen: European Environment Agency, 2002.](#)

546

547 Camarasa-Belmonte, A.M.: Flash floods in Mediterranean ephemeral streams in Valencia Region, *J.*  
548 *Hydrol.*, 541, 99–115, 2016.

549

550 Camici, S., Brocca, L., and Moramarco, T.: Accuracy versus variability of climate projections for flood  
551 assessment in central Italy, *Climatic Change* 141(2), 273-286, 2017.

552

553 CCR 2018. Conséquences du changement climatique sur les coûts des catastrophes naturelles en France à  
554 Horizon 2050.  
555 [https://www.ccr.fr/documents/23509/29230/Etude+Climatique+2018+version+complete.pdf/6a7b6120-](https://www.ccr.fr/documents/23509/29230/Etude+Climatique+2018+version+complete.pdf/6a7b6120-7050-ff2e-4aa9-89e80c1e30f2)  
556 [7050-ff2e-4aa9-89e80c1e30f2](https://www.ccr.fr/documents/23509/29230/Etude+Climatique+2018+version+complete.pdf/6a7b6120-7050-ff2e-4aa9-89e80c1e30f2)

557

558 Dayon, G., Boé, J., Martin, E., and Gailhard, J.: Impacts of climate change on the hydrological cycle over  
559 France and associated uncertainties, *Comptes Rendus Geosciences*, 350(4), 141-153, 2018.

560  
561 Do, H.X., Westra, S., and Leonard, M.: A global-scale investigation of trends in annual maximum  
562 streamflow, *J. Hydrol.*, 552, 28–43, 2017.

563  
564 Donnelly, C., Greuell, W., Andersson, J., Gerten, D., Pisacane, G., Roudier, P., and Ludwig, F.: Impacts  
565 of climate change on European hydrology at 1.5, 2 and 3 degrees mean global warming above  
566 preindustrial level, *Climatic Change*, 19, 1–14, 2017.

567  
568 [Drobinski, P., Alonzo, B., Bastin, S., Silva, N. D., and Muller, C.: Scaling of precipitation](#)  
569 [extremes with temper-ature in the French Mediterranean region: what explainsthe hook shape?.](#)  
570 [J. Geophys. Res.-Atmos., 121, 3100–3119,https://doi.org/10.1002/2015JD023497, 2016](#)

571  
572 Efron, B.: Bootstrap Methods: Another Look at the Jackknife, *Ann. Stat.*, 7, 1–26, 1979.

573  
574 Giuntoli, I., Renard, B., and Lang, M.: Floods in France. In: Z.W. Kundzewicz, ed. Changes in flood risk  
575 in Europe. Wallingford, UK: IAHS and CRC/Balkema, IAHS Special Publ. 10, 212–224, 2012.

576  
577 Grillakis, M.G., Koutroulis, A.G., Komma, J., Tsanis, I.K., Wagner, W., and Blöschl, G.: Initial  
578 soil moisture effects on flash flood generation - A comparison between basins of contrasting  
579 hydro-climatic conditions, *Journal of Hydrology* 541, 206-217, 2016.

580  
581 Habets, F., Boone, A., Champeaux, J.-L., Etchevers, P., Franchis-teguy, L., Leblois, E., Ledoux, E., Le  
582 Moigne, P., Martin, E., Morel, S., Noilhan, J., Quintana-Segui, P., Rousset-Regimbeau, F., and Viennot,  
583 P.: The SAFRAN-ISBA-MODCOU hydrometeorological model applied over France, *J. Geophys. Res.*,  
584 113, D06113, doi:10.1029/2007JD008548, 2008.

585  
586 Hamed, K.H. and Rao, A.R.: A modified Mann-Kendall trend test for autocorrelated data, *J. Hydrol.*, 204,  
587 182–196, 1998.

588  
589 Hodgkins, G. A., Whitfield, P. H., Burn, D. H., Hannaford, J., Renard, B., Stahl, K., Fleig, A. K.,  
590 Madsen, H., Mediero, L., Ko-rhonen, J., Murphy, C., and Wilson, D.: Climate-driven variability in the  
591 occurrence of major floods across North America and Europe, *J. Hydrol.*, 552, 704–717, 2017.

592

593 Ivancic, T.J., Shaw S.B.: Examining why trends in very heavy precipitation should not be mistaken for  
594 trends in very high river discharge, *Climatic Change*, 133, 681-693, 2015.  
595

596 Jourde, H., Roesch, A., Guinot, V. and Bailly-Comte, V.: Dynamics and contribution of karst  
597 groundwater to surface flow during Mediterranean flood, *Environmental Geology*, 51, 725–730, 2007.  
598

599 Khaliq, M.N., Ouarda, T.B.M.J, Gachon, P., Sushama, L., and St-Hilaire, A.: Identification of  
600 hydrological trends in the presence of serial and cross correlations: A review of selected methods and  
601 their application to annual flow regimes of Canadian rivers, *J. Hydrol.*, 368, 117–130, 2009.  
602

603 Knighton, J.O., DeGaetano, A., and Walter, M.T.: Hydrologic state influence on riverine flood discharge  
604 for a small temperate watershed (Fall Creek, United States): negative feedbacks on the effects of climate  
605 change, *J. Hydrometeorol.*, 18(2), 431–449, 2017.  
606

607 Koenker, R. and Basset, B.G.: Regression quantiles, *Econometrica*, 46(1), 33–50, 1978.  
608

609 Koenker, R., Machado J.A.F.: Goodness-of-fit and related inference processes for quantile regression,  
610 *Journal of the American Statistical Association*, 94(448), 1296–1310, 1999.  
611

612 Kundzewicz, Z.W., Krysanova, V., Dankers, R., Hirabayashi, Y., Kanae, S., Hattermann, F.F., Huang, S.,  
613 Milly, P.C.D., Stoffel, M., Driessen, P.P.J., Matczak, P., Quevauviller, P., and Schellnhuber, H.-J.:  
614 Differences in flood hazard projections in Europe – their causes and consequences for decision making,  
615 *Hydrological Sciences Journal*, 62(1), 1-14, 2017.  
616

617 Llasat, M.C., Llasat-Botija, M., Petrucci, O., Pasqua, A. A., Rosselló, J., Vinet, F., and Boissier, L.:  
618 Towards a database on societal impact of Mediterranean floods within the framework of the HYMEX  
619 project, *Nat. Hazards Earth Syst. Sci.*, 13, 1337-1350, 2013.  
620

621 Mann, H. B.: Nonparametric tests against trend, *Econometrica*, 13,245– 259, 1945  
622

623 Mangini, W., Viglione, A., Hall, J., Hundecha, Y., Ceola, S., Montanari, A., Rogger, M., Salinas, J.L.,  
624 Borzi, I., and Parajka, J.: Detection of trends in magnitude and frequency of flood peaks across Europe,  
625 *Hydrological Sciences Journal*, 63(4), 493-512, 2018.  
626

627 Mediero, L., Santillán, D., Garrote, L., and Granados, A.: Detection and attribution of trends in magnitude,  
628 frequency and timing of floods in Spain, *J. Hydrol.*, 517, 1072–1088, 2014.

629

630 Merz, B., Aerts, J., Arnbjerg-Nielsen, K., Baldi, M., Becker, A., Bichet, A., Blöschl, G., Bouwer, L. M.,  
631 Brauer, A., Cioffi, F., Delgado, J. M., Gocht, M., Guzzetti, F., Harrigan, S., Hirschboeck, K., Kilsby, C.,  
632 Kron, W., Kwon, H.-H., Lall, U., Merz, R., Nissen, K., Salvatti, P., Swierczynski, T., Ulbrich, U.,  
633 Viglione, A., Ward, P. J., Weiler, M., Wilhelm, B., and Nied, M.: Floods and climate: emerging  
634 perspectives for flood risk assessment and management, *Nat. Hazards Earth Syst. Sci.*, 14, 1921-1942,  
635 2014.

636

637 Meyer, V., Becker, N., Markantonis, V., Schwarze, R., van den Bergh, J. C. J. M., Bouwer, L. M.,  
638 Bubeck, P., Ciavola, P., Genovese, E., Green, C., Hallegatte, S., Kreibich, H., Lequeux, Q., Logar, I.,  
639 Papyrakis, E., Pfurtscheller, C., Poussin, J., Przyluski, V., Thielen, A. H., and Viavattene, C.: Review  
640 article: Assessing the costs of natural hazards – state of the art and knowledge gaps, *Nat. Hazards Earth*  
641 *Syst. Sci.*, 13, 1351-1373, <https://doi.org/10.5194/nhess-13-1351-2013>, 2013.

642

643 Najibi, N. and Devineni, N.: Recent trends in the frequency and duration of global floods, *Earth Syst.*  
644 *Dynam.*, 9, 757-783, 2018.

645

646 Neppel L., Bouvier C., Desbordes M., and Vinet F.: A possible origin for the increase in floods in the  
647 Mediterranean region. *Revue des sciences de l'eau* 16(4), 389-494, 2003.

648

649 Norbiato, D., Borga, M., Esposti, S.D., Gaume, E., and Anquetin, S.: Flash flood warning based on  
650 rainfall thresholds and soil moisture conditions: An assessment for gauged and ungauged basins, *Journal*  
651 *of Hydrology*, 362, 274-290, 2008.

652

653 ~~Penna, D., Tromp-van Meerveld, H.J., Gobbi, A., Borga, M., and Dalla Fontana, G.: The influence of soil~~  
654 ~~moisture on threshold runoff generation processes in an alpine headwater catchment, *Hydrology and Earth*~~  
655 ~~*System Sciences*, 15, 689-702, 2011.~~

656

657 Paprotny, D., Sebastian, A., Morales-Nápoles, O., and Jonkman, S. N.: Trends in flood losses in Europe  
658 over the past 150 years, *Nature Communications*, 9(1),1985, doi:10.1038/s41467-018-04253-1, 2018.

659

660 [Paxian, A., Hertig, E., Seubert, S., Vogt, G., Jacobeit, J., and Paeth, H.: Present-day and future](#)  
661 [Mediterranean precipitation extremes assessed by different statistical approaches, \*Clim. Dynam.\*, 44, 845–](#)  
662 [860, <https://doi.org/10.1007/s00382-014-2428-6>, 2015](#)

663

664 [Penna, D., Tromp-van Meerveld, H.J., Gobbi, A., Borga, M., and Dalla Fontana, G.: The influence of soil](#)  
665 [moisture on threshold runoff generation processes in an alpine headwater catchment, \*Hydrology and Earth\*](#)  
666 [System Sciences](#), 15, 689–702, 2011.

667

668 Petrucci, O., Papagiannaki, K., Aceto, L., Boissier, L., Kotroni, V., Grimalt, M., Llasat, M. C.,  
669 Llasat-Botija, M., Rosselló, J., Pasqua, A. A., and Vinet, F.: MEFF: The database of Mediterranean  
670 Flood Fatalities (1980 to 2015), *J. Flood Risk Manage.*, e12461, <https://doi.org/10.1111/jfr3.12461>, 2018.

671

672 [Pfahl, S., O’Gorman, P. A., and Fischer, E. M.: Understanding the regional pattern of](#)  
673 [projected future changes in extreme precipitation, \*Nat. Clim. Change\*, 7, 423–](#)  
674 [427, <https://doi.org/10.1038/nclimate3287>, 2017.](#)

675

676 Piras, M., Mascaro, G., Deidda, R., and Vivoni, E.R.: Impacts of climate change on precipitation and  
677 discharge extremes through the use of statistical downscaling approaches in a Mediterranean basin,  
678 *Sci. Total Environ.*, 543, 952–964, 2016.

679

680 [Polade, S. D., Pierce, D. W., Cayan, D. R., Gershunov, A. and Dettinger, M. D.: The key role of dry days](#)  
681 [in changing regional climate and precipitation regimes, \*Sci. Rep.\* 4, 4364, 2014.](#)

682

683 Polade, S.D., Gershunov, A., Cayan, D.R., Dettinger, M.D., and Pierce, D.W.: Precipitation in a warming  
684 world: Assessing projected hydro-climate changes in California and other Mediterranean climate regions,  
685 *Scientific Reports* 7, 10783, doi:10.1038/s41598-017-11285-y, 2017.

686

687 Quintana-Seguí, P., Habets, F., and Martin, E.: Comparison of past and future Mediterranean high and low  
688 extremes of precipitation and river flow projected using different statistical downscaling methods, *Nat.*  
689 *Hazards Earth Syst. Sci.*, 11, 1411–1432, 2011.

690

691 Quintana-Seguí, P., Le Moigne, P., Durand, Y., Martin, E., Habets, F., Baillon, M., Canellas, C.,  
692 Franchisteguy, L., and Morel, S.: Analysis of Near-Surface Atmospheric Variables : Validation of the  
693 SAFRAN Analysis over France, *J. Appl. Meteor. Climatol.*, 47, 92–107, 2008.

694  
695 Raynaud, D., Thielen, J., Salamon, P., Burek, P., Anquetin, S., and Alfieri, L.: A dynamic runoff  
696 coefficient to improve flash flood early warning in Europe: validation on the 2013 Central Euro-pean  
697 floods in Germany. *Met. Apps*, 22: 410-418, 2015.  
698  
699 Renard, B., Lang, M., Bois, P., Dupeyrat, A., Mestre, O., Niel, H.,Sauquet, E., Prudhomme, C., Parey, S.,  
700 Paquet, E., Neppel, L.,and Gailhard, J.: Regional methods for trend detection: assessingfield significance  
701 and regional consistency, *Water Resour. Res.*,44, W08419, doi:10.1029/2007WR006268, 2008.  
702  
703 Ribes, A., Soulivanh, T., Vautard, R., Dubuisson, B., Somot, S., Colin, J., Planton, S., and Soubeyroux, J-  
704 M. : Observed increase in extreme daily rainfall in the French Mediterranean. *Clim Dyn.* 52, 1095-1114,  
705 2019.  
706  
707 [Rivoire, P., Tramblay, Y., Neppel, L., Hertig, E., and Vicente-Serrano, S. M.: Impact of the dry-day](#)  
708 [definition on Mediterranean extreme dry-spell analysis, \*Nat. Hazards Earth Syst. Sci.\*, 19, 1629–1638,](#)  
709 <https://doi.org/10.5194/nhess-19-1629-2019>, 2019. ~~Rivoire, P., Tramblay, Y., Neppel, L., Hertig, E., and~~  
710 ~~Vicente-Serrano, S. M.: Impact of the dry-day definition on Mediterranean extreme dry spells analysis,~~  
711 ~~*Nat. Hazards Earth Syst. Sci. Discuss.*, <https://doi.org/10.5194/nhess-2019-31>, in review, 2019.~~  
712  
713 Ruin, I., Creutin, J.-D., Anquetin, S. and Lutoff, C.: Human exposure to flash-floods - Relation between  
714 flood parameters and human vulnerability during a storm of September 2002 in southern France,  
715 *J. Hydrol.*, 361, 199-213, 2008.  
716  
717 Saint-Martin, C., Javelle, P., and Vinet, F.: DamaGIS: a multisource geodatabase for collection of flood-  
718 related damage data, *Earth Syst. Sci. Data*, 10, 1019-1029, <https://doi.org/10.5194/essd-10-1019-2018>,  
719 2018.  
720  
721 Sauquet, E. and Catalogne, C.: Comparison of catchment grouping methods for flow duration curve  
722 estimation at ungauged sites in France, *Hydrol. Earth Syst. Sci.*, 15, 2421-2435,  
723 <https://doi.org/10.5194/hess-15-2421-2011>, 2011.  
724  
725 Sen, P.K.: Estimates of the regression coefficient based on Kendall's tau, *J. Am. Stat. Assoc.*,  
726 63, 1379–1389, 1968  
727

728 Schomburgk S., Allier D., and Seguin J.J.: The new aquifer Reference system BDLISA in France and the  
729 representation of karst units : challenges of small-scale mapping, in *Grundwasser - Mensch - Ökosysteme*.  
730 25. Tagung des Fachsektion Hydrogeologie in der DGGV 2016, Karlsruher Institut für Technologie  
731 (KIT), 13. -17. April 2016, Germany. KIT Scientific Publishing. n° ISBN : 978-3-7315-0475-7, 2016.  
732

733 Sharma, A., Wasko, C., & Lettenmaier, D.P.: If precipitation extremes are increasing, why aren't floods?  
734 *Water Resources Research*, 54, 8545–8551, 2018.  
735

736 Snelder, T. H., Datry, T., Lamouroux, N., Larned, S. T., Sauquet, E., Pella, H., and Catalogne, C.:  
737 Regionalization of patterns of flow intermittence from gauging station records, *Hydrol. Earth Syst. Sci.*,  
738 17, 2685-2699, <https://doi.org/10.5194/hess-17-2685-2013>, 2013.  
739

740 Thober, S., Kumar, R., Wanders, N., Marx, A., Pan, M., Rakovec, O., Samaniego, L., Sheffield, J.,  
741 Wood, E. F., and Zink, M.: Multi-model ensemble projections of European river floods and high flows  
742 at 1.5, 2, and 3 degree global warming, *Environ. Res. Lett.*, 13, 1–22, 2018.  
743

744 Tramblay Y., Somot S.: Future evolution of extreme precipitation in the Mediterranean, *Climatic Change*  
745 151(2), 289–302, 2018.  
746

747 Tramblay, Y., Neppel, L., Carreau, J., and Najib, K.: Non-stationary frequency analysis of heavy rainfall  
748 events in southern France, *Hydrol. Sci. J.*, 58, 1–15, 2013.  
749

750 Tramblay, Y., Bouvier, C., Martin, C., Didon-Lescot, J.F., Todorovik, D., and Domergue, J. M.:  
751 Assessment of initial soil moisture conditions for event-based rainfall-runoff modelling, *J. Hydrol.*, 387,  
752 176-187, 2010.  
753

754 Uber, M., Vandervaere, J.-P., Zin, I., Braud, I., Heistermann, M., Legout, C., Molinié, G., and Nord, G.:  
755 How does initial soil moisture influence the hydrological response? A case study from southern France,  
756 *Hydrol. Earth Syst. Sci.*, 22, 6127-6146, <https://doi.org/10.5194/hess-22-6127-2018>, 2018.  
757

758 Vicente-Serrano, S.M., Azorin-Molina, C., Sanchez-Lorenzo, A., Revuelto, J., López-Moreno, J.I.,  
759 González-Hidalgo, J.C., and Espejo, F.: Reference evapotranspiration variability and trends in Spain,  
760 1961–2011. *Global and Planetary Change*, 121, 26–40, 2014.  
761



762 Vidal, J.-P., Martin, E., Kitova, N., Najac, J., and Soubeyroux, J.-M.: Evolution of spatio-temporal  
763 drought characteristics: validation, projections and effect of adaptation scenarios, *Hydrol. Earth Syst. Sci.*,  
764 16, 2935-2955, <https://doi.org/10.5194/hess-16-2935-2012>, 2012.

765

766 Viglione, A., Merz, R., and Blöschl, G.: On the role of the runoff coefficient in the mapping of rainfall to  
767 flood return periods, *Hydrol. Earth Syst. Sci.*, 13, 577-593, <https://doi.org/10.5194/hess-13-577-2009>,  
768 2009.

769

770 Villarini G. and Slater L.: Examination of Changes in Annual Maximum Gauge Height in the Continental  
771 United States Using Quantile Regression. *J. Hydrol. Eng.*, DOI:10.1061/(ASCE)HE.1943-5584.0001620,  
772 2017.

773

774 Vinet, F.: Flood Risk Assessment and Management in France. The Case of Mediterranean Basins, *Flood*  
775 *Prevention and Remediation*. WIT Press, Southampton, UK, p. 105–132, 2011.

776

777 Vinet F. and Meschinet de Richemond N.: Changes in Flood Risk: Retrospective and Prospective  
778 Approach, Chap. 14 in F. VINET (ed.) *Floods 1: risk knowledge* ISTE edition London, p. 311-323, 2017.

779

780 [Wasko C., Parinussa R.M., and Sharma A.: A quasi-global assessment of changes in remotely sensed](#)  
781 [rainfall extremes with temperature, \*Geophys Res Lett\* 43:12, 659–612.668, 2016.](#)

782

783 Wasko, C. and Sharma, A.: Global assessment of flood and storm extremes with increased temperatures,  
784 *Sci Rep*, 7(1), 7945, doi:10.1038/s41598-017-08481-1, 2017.

785

786 Wasko C. and Nathan R.: Influence of changes in rainfall and soil moisture on trends in flooding, *J.*  
787 *Hydrol.*, 575, 432-441, 2019.

788

789 Westra, S., Alexander, L. V., and Zwiers, F. W.: Global increasing trends in annual maximum daily  
790 precipitation, *J. Climate*, 26, 3904–3918, 2013

791

792 Whitfield, P.: Changing floods in future climates. *J. Flood Risk Manage*, 5: 336-365, 2012.

793

794 Wilks, D.S.: The stippling shows statistically significant grid points: how research results are routinely  
795 overstated and over interpreted, and what to do about it, *Bull. Am. Meteorol. Soc.*, 97, 2263–2273, 2016.

796  
797 Woldemeskel, F. and Sharma, A.: Should flood regimes change in a warming climate? The role of  
798 antecedent moisture conditions, *Geophys. Res. Lett.*, 43, 7556–7563, doi:10.1002/2016GL069448, 2016.  
799  
800 Yin, J., Gentile, P., Zhou, S., Sullivan, S.C., Wang, R., Zhang, Y., and Guo, S.: Large increase in global  
801 storm runoff extremes driven by climate and anthropogenic changes. *Nat. Commun.* 9, 4389,  
802 DOI:10.1038/s41467-018-06765-2, 2018.  
803  
804 Zhang, Y., Wei, H., and Nearing, M. A.: Effects of antecedent soil moisture on runoff modeling in small  
805 semiarid watersheds of southeastern Arizona, *Hydrol. Earth Syst. Sci.*, 15, 3171-3179,  
806 <https://doi.org/10.5194/hess-15-3171-2011>, 2011.  
807  
808  
809  
810  
811  
812  
813  
814  
815  
816  
817  
818  
819  
820  
821  
822  
823  
824  
825  
826  
827

828  
829  
830

**Table 1:** summary of the trend detection on different variables: number of positive, negative trends significant at the 10% level and regional significance

Mis en forme : Police :Gras

	<u>Variable</u>	<u>Positive trends</u>	<u>Negative trends</u>	<u>Regional significance</u>
<u>Climatic variables</u>	<u>Mean precipitation</u>	<u>0</u>	<u>56</u>	<u>Yes (28 basins)</u>
	<u>Mean rainfall</u>	<u>1</u>	<u>49</u>	<u>Yes (20 basins)</u>
	<u>Frequency of dry days</u>	<u>46</u>	<u>2</u>	<u>Yes (9 basins)</u>
	<u>Mean temperature</u>	<u>166</u>	<u>0</u>	<u>Yes (165 basins)</u>
	<u>Mean surface soil moisture</u>	<u>1</u>	<u>132</u>	<u>Yes (129 basins)</u>
	<u>Mean root zone soil moisture</u>	<u>1</u>	<u>132</u>	<u>Yes (129 basins)</u>
	<u>Mean actual evapotranspiration</u>	<u>169</u>	<u>0</u>	<u>Yes (169 basins)</u>
	<u>Mean reference evapotranspiration</u>	<u>136</u>	<u>0</u>	<u>Yes (131 basins)</u>
<u>Flood events</u>	<u>Number of floods above the 95th percentile</u>	<u>0</u>	<u>67</u>	<u>Yes (40 basins)</u>
	<u>Number of floods above the 99th percentile</u>	<u>1</u>	<u>45</u>	<u>Yes (7 basins)</u>
	<u>Flood magnitudes above the 95th percentile</u>	<u>4</u>	<u>3</u>	<u>No</u>
	<u>Flood magnitudes above the 99th percentile</u>	<u>16</u>	<u>5</u>	<u>No</u>
<u>Climatic variables associated with flood events</u>	<u>Cumulative precipitation during floods above the 95th percentile</u>	<u>36</u>	<u>6</u>	<u>Yes (16 basins)</u>
	<u>Cumulative precipitation during floods above the 99th percentile</u>	<u>34</u>	<u>3</u>	<u>Yes (5 basins)</u>
	<u>Antecedent wetness conditions for floods above the 95th percentile</u>	<u>10</u>	<u>40</u>	<u>Yes (11 basins)</u>
	<u>Antecedent wetness conditions for floods above the 95th percentile</u>	<u>6</u>	<u>24</u>	<u>Yes (14 basins)</u>

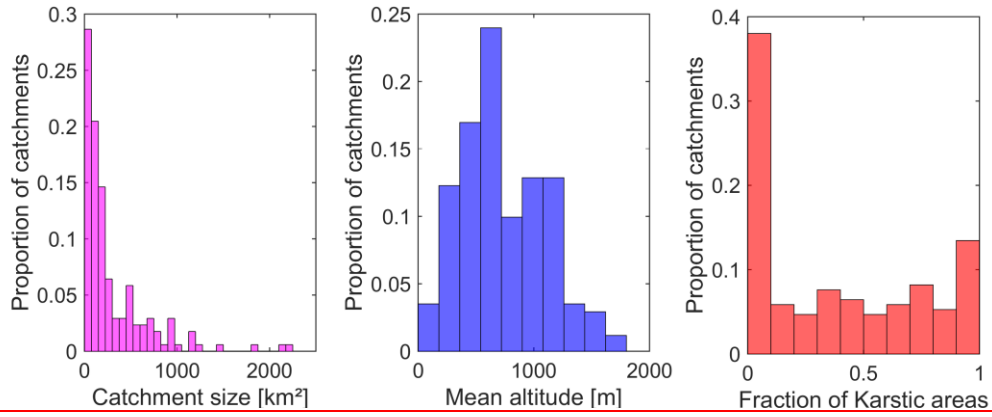
Mis en forme : Anglais (États Unis)

831  
832  
833  
834  
835  
836  
837  
838

839 **FIGURES**

840

841



842

843

844 Figure 1: Catchment size, mean altitude and fraction of karstic areas

845

846

847

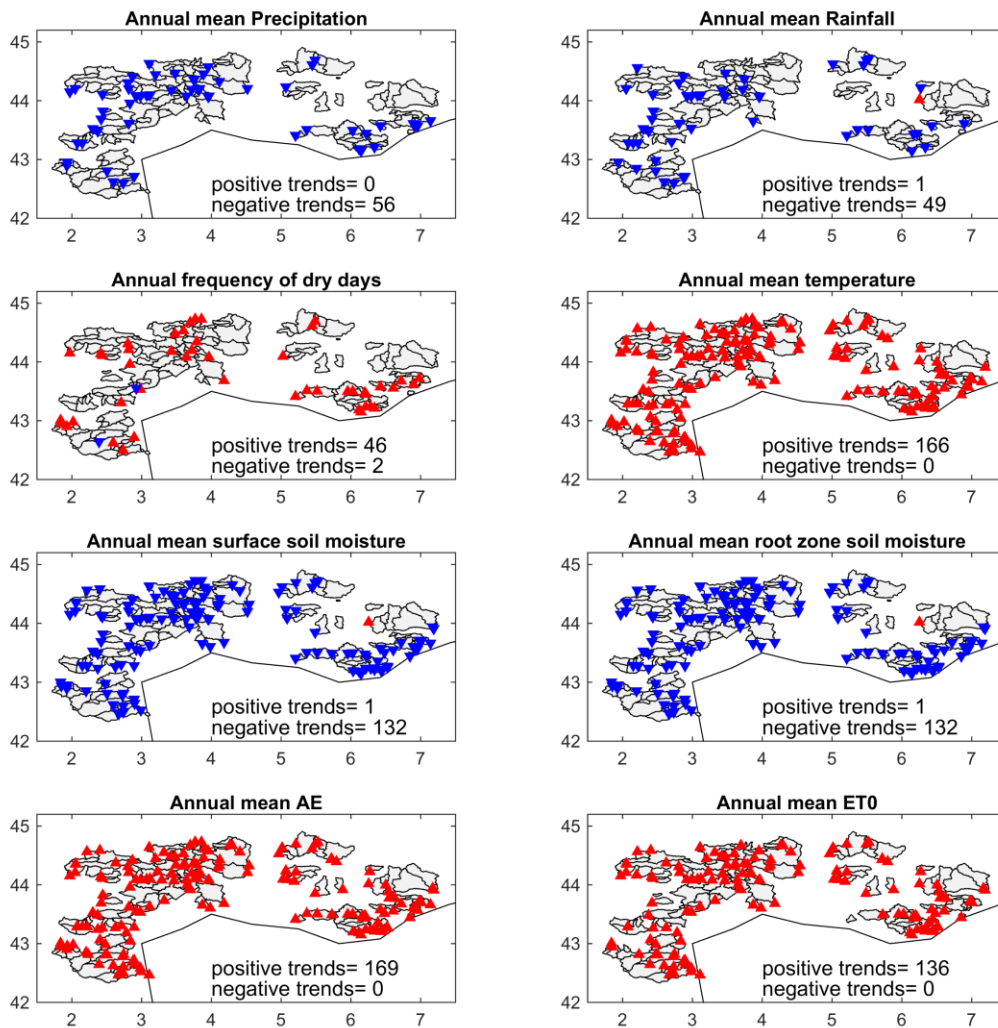
848

849

850

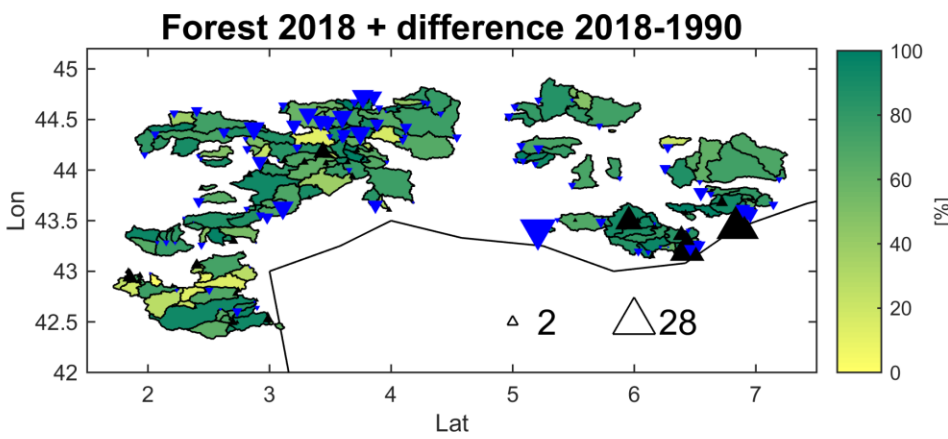
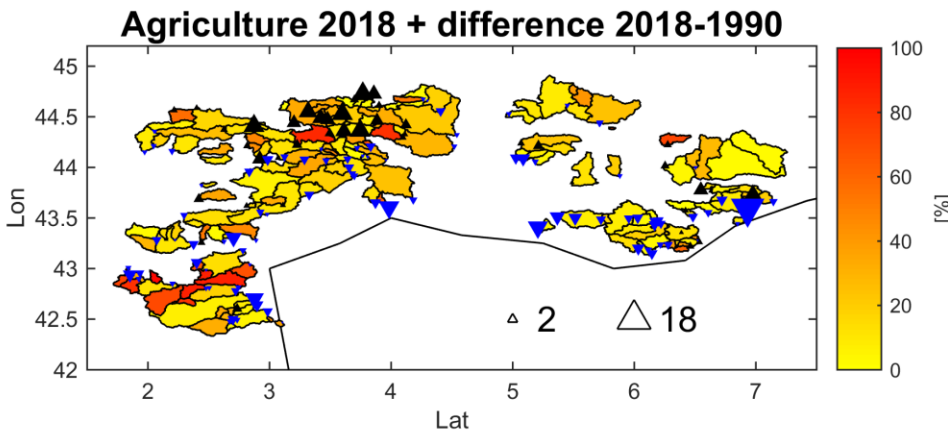
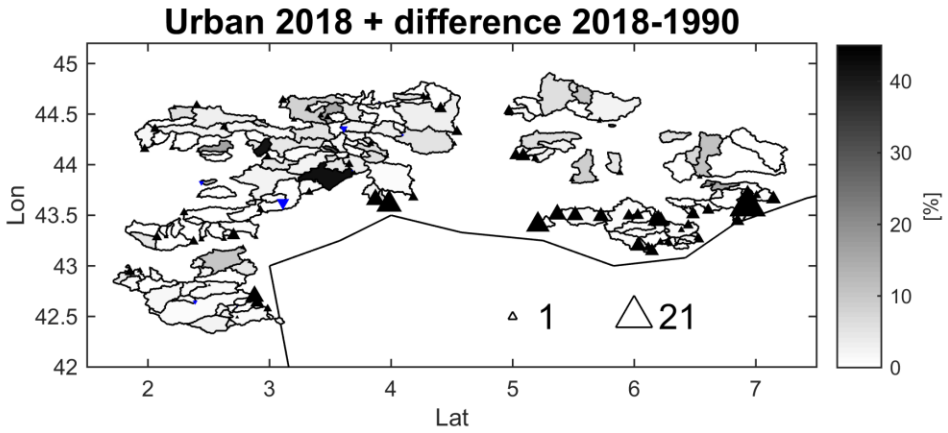
851

852



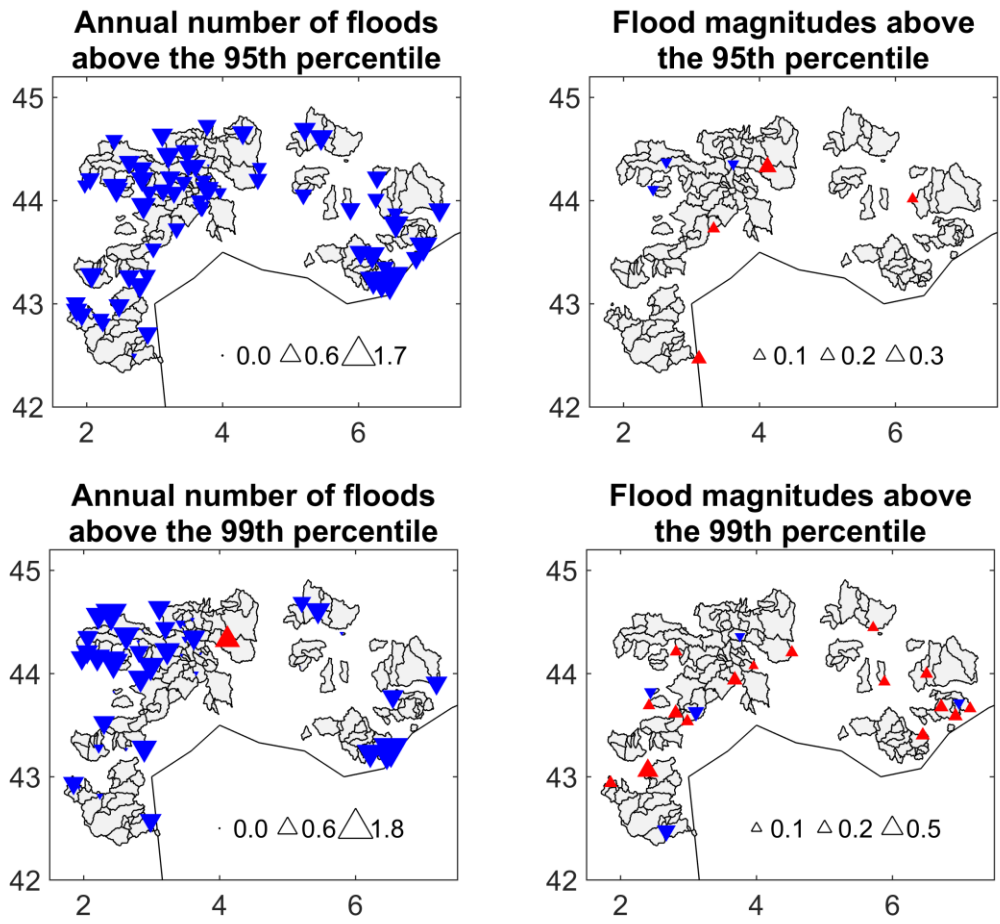
853  
 854  
 855  
 856  
 857  
 858  
 859  
 860

Figure 2: Significant annual trends at the 10% level (Mann Kendall test) between 1958 and 2018 in precipitation, rainfall, frequency of dry days (with precipitation below 1mm), temperature, soil moisture, actual evapotranspiration (AE) and reference evapotranspiration (ET0)



863  
864  
865  
866  
867  
868  
869  
870  
871  
872  
873  
874  
875  
876  
877  
878

Figure 3: Urban, Agricultural and Forest cover by catchment from the CORINE database for the year 2018 and difference between 1990 and 2018 (upward black triangles indicate an increase, downward blue triangles a decrease, the triangle size are proportional to the absolute changes between 1990 and 2018).

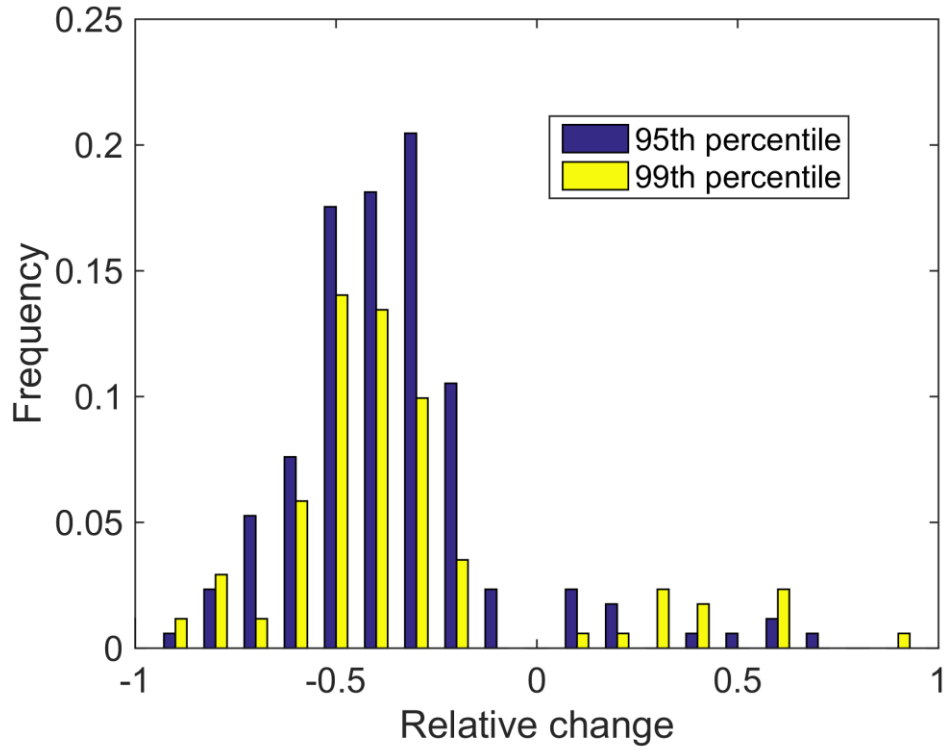


879  
880  
881  
882  
883  
884  
885  
886  
887  
888  
889

Figure 4: Significant trends at the 10% level (Mann Kendall test) Trends in the annual number of flood events above the 95<sup>th</sup> and 99<sup>th</sup> percentiles (left) and in the magnitude of these threshold exceedances (right). Blue triangles indicate a decrease and red triangles an increase. The size of the triangles indicates the relative changes.



890  
891  
892

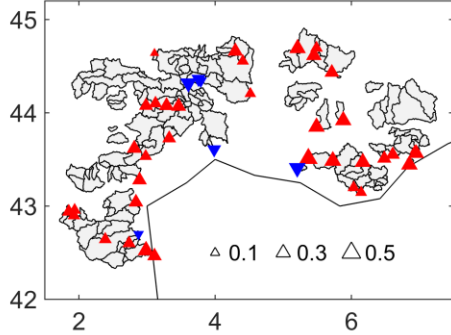


893  
894  
895

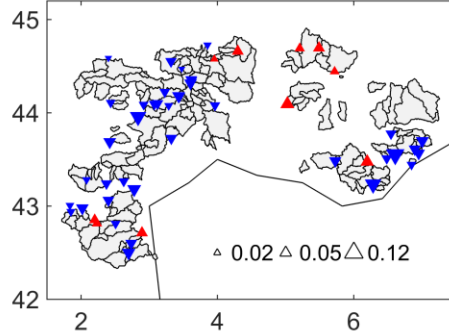
896 Figure 5: Histogram of the relative changes in the 95<sup>th</sup> and 99<sup>th</sup> percentiles estimated from the  
897 quantile regression models with time as covariate (with a slope significantly different than zero at  
898 the 10% level)

899  
900  
901  
902  
903  
904

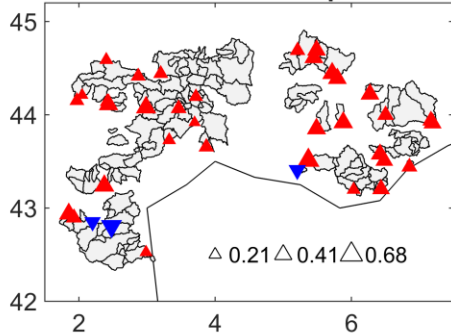
**Cumulative precipitation during floods above the 95th percentile**



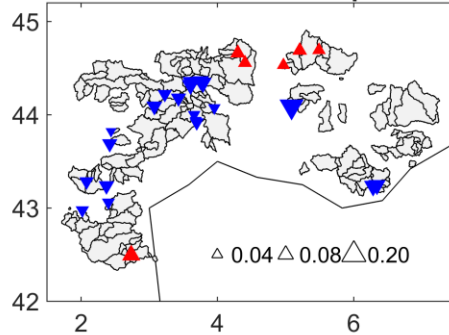
**Antecedent wetness conditions for floods above the 95th percentile**



**Cumulative precipitation during floods above the 99th percentile**



**Antecedent wetness conditions for floods above the 99th percentile**



905

906

907

908

909

910

911

912

913

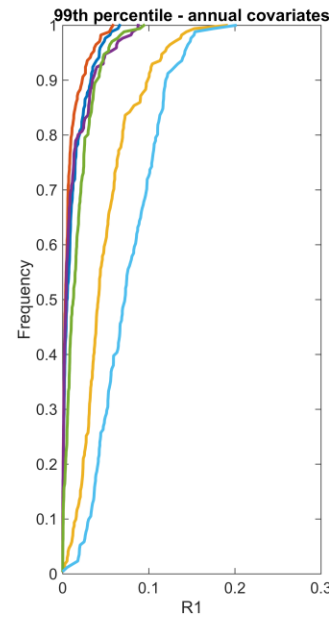
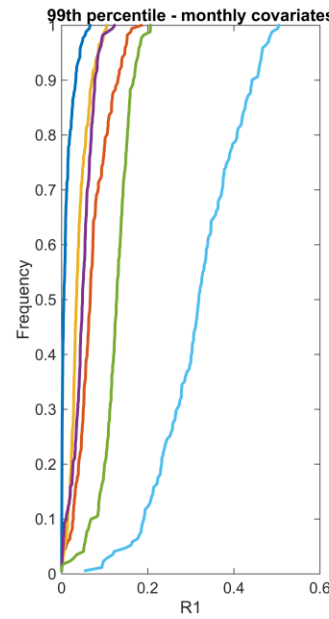
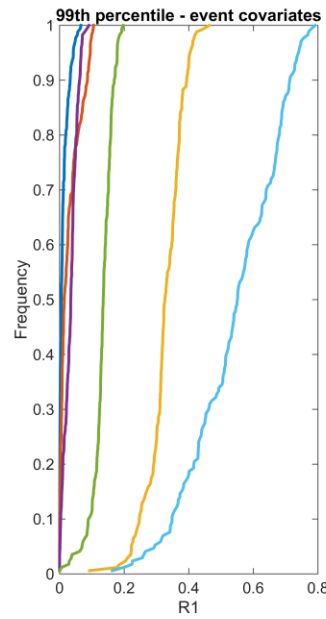
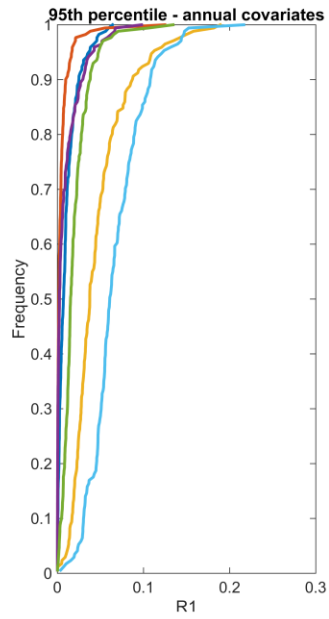
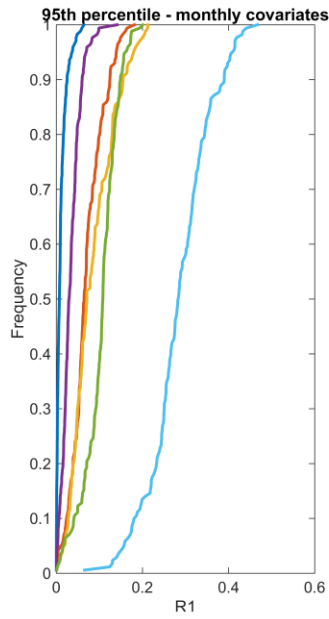
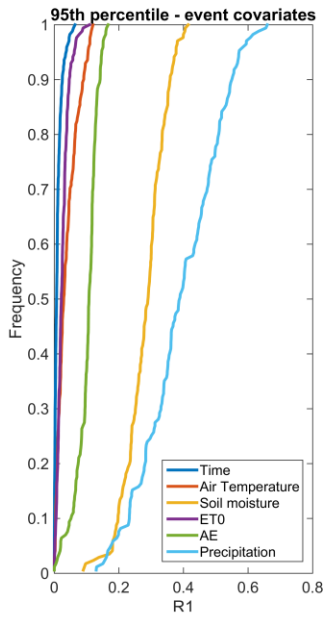
914

915

916

917

Figure 6: Significant trends at the 10% level (Mann Kendall test) Trends in cumulative precipitation during flood events above the 95<sup>th</sup> and 99<sup>th</sup> percentile (left) and in the soil moisture initial conditions (right). Blue triangles indicate a decrease and red triangles an increase. The size of the triangles indicates the relative changes.



918

919

920 Figure 7: Distribution of the  $R^l$  coefficients for different covariates for the 95<sup>th</sup> or 99<sup>th</sup> percentiles  
921 of daily runoff, averaged at: (i) the event scale (3 days), left panels, (ii) the monthly scale, central  
922 panels, and (ii) annual timescale, right panels.  
923